

# Underwater SLAM with Robocentric Trajectory Using a Mechanically Scanned Imaging Sonar

Antoni Burguera, Yolanda González and Gabriel Oliver

**Abstract**—This paper proposes a novel approach to perform underwater *Simultaneous Localization and Mapping* (SLAM) using a *Mechanically Scanned Imaging Sonar* (MSIS). This approach starts by processing the MSIS data in order to obtain range scans while taking into account the robot motion. Then, the relative motions between consecutively gathered scans are stored in the state vector. Thus, the whole sequence of robot motions between gathered scans is used to perform SLAM using an *Extended Kalman Filter* (EKF). One of the novelties is that this sequence is not represented with respect to a world-fixed coordinate frame, but with respect to a coordinate frame locked to the robot. Thanks to this, EKF linearization errors are reduced. The experimental results in underwater environments validate the proposal comparing the new robocentric approach to the world-centric trajectory method.

## I. INTRODUCTION

Keeping track of the robot position is a crucial issue in most mobile robotic applications nowadays. The *Simultaneous Localization and Mapping* (SLAM) approach [1] has proved to be a reliable solution, allowing to obtain accurate pose estimates even in long-term missions.

The first attempts to perform SLAM were based on the *Extended Kalman Filter* (EKF). In spite of its great success, the robotics community soon realized that the linearization errors introduced by EKF could not be neglected as they lead the SLAM estimates to inconsistencies [2].

Other bayesian methods [3], such as *Particle Filtering*, are widely used by the SLAM community. However, the EKF approach is still the most popular one because of its conceptual simplicity and relatively low computational cost. At the present time, research in EKF-SLAM is focused on reducing the linearization errors so that long term missions can be successfully achieved.

It is well known that linearization errors become larger when large covariances are involved. Approaches such as *hierarchical SLAM* or *submapping* methods [4], [5] build local maps of limited size, which bound the covariances and, thus, the linearization errors. Then, by linking the local maps through a global map or a hierarchy of global maps, EKF-SLAM in large environments is possible.

Another approach, the *robocentric SLAM* [6], is concerned with the increase of covariances with the distance from the robot starting pose. To alleviate this problem, it proposes an alternative representation where the map is always represented with respect to the robot itself. In this way, the

covariances of the features close to the robot, which are those involved in the data association and the EKF measurement update, are small and bounded. Robocentric SLAM has also been successfully combined with submapping techniques [7].

The *Trajectory-based SLAM* [8] has some points in common with submapping techniques. In this approach, the EKF state vector contains the relative robot motions between consecutively gathered sensor scans. Because of the local representation, the filter always operates on small and bounded covariances. When a new range scan is gathered, it is matched against the existing ones using scan matching techniques and the EKF correction is applied to each involved local motion. In this way, the correction is performed at the trajectory level, instead of solely correcting the current robot pose.

However, due to the trajectory representation, the linearization errors increase with the proximity of the matched scan to the current one. This produces some problems, because matchings with close scans will appear during the most part of the robot operation, whilst matchings involving far scans will appear rarely. Moreover, matching between close scans is more reliable than between far scans. Accordingly, reducing the linearization errors for those matchings involving scans close to the robot would increase the quality of the pose estimates. This goal is similar to the one of Robocentric SLAM, and it is clear that the Trajectory-based approach can benefit from Robocentric SLAM one.

This work is focused on underwater robotics. When comparing to terrestrial applications, underwater robotics poses additional problems, mainly related to the robot sensing capabilities. In our particular implementation, a *Mechanically Scanned Imaging Sonar* (MSIS) has been used to observe the environment. This kind of sensors has two problems when it is used to perform SLAM based on range scans. First, it does not provide range measurements but echo intensity profiles. In addition, due to the acoustic beam's opening, and also to the multi-path reflections, an echo intensity profile may contain more than one peak. Second, as the sensor is mechanically scanned, the scan gathering time is not negligible. In particular, gathering a full scan may take a few seconds, which means that the robot motion during the data gathering has to be taken into account.

This paper is concerned with the aforementioned problems in underwater environments: how to obtain range information from the MSIS echo intensity profiles, how to compensate the robot motion during the data gathering by means of a *Doppler Velocity Log* (DVL) sensor and finally a new robocentric trajectory approach to underwater SLAM that

This work is partially supported by DPI 2008-06548-C03-02, FEDER funding and FP7-TRIDENT Project SCP8-GA-2010-248497.

Dept. Matemàtiques i Informàtica. Universitat de les Illes Balears. Ctra. Valldemossa Km. 7,5. 07122 Palma de Mallorca (SPAIN) {antoni.burguera, y.gonzalez, goliver}@uib.es

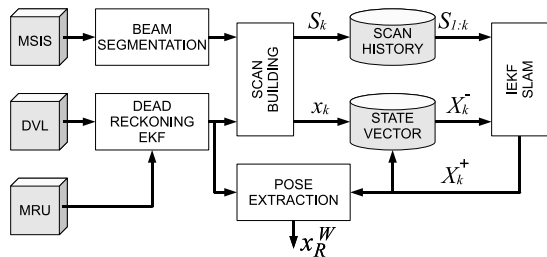


Fig. 1. Overview of the scan-based SLAM. The notation is explained throughout the paper.

overcomes the limitations of the trajectory based SLAM is presented.

The problem is summarized in section II, where also the beam segmentation and the scan building processes are introduced. Section III summarizes the world-centric scan based SLAM. And in section IV the new robocentric trajectory SLAM approach is described. The experimental results are provided in section V. The results, which are based on real data gathered by an AUV, show the benefits of the presented approach by comparing it with world-centric method. Section VI concludes the paper.

## II. PROBLEM STATEMENT

The experiments conducted in this paper have been performed using the sensor data gathered by the *Ictineu* AUV. This AUV was designed and developed at the University of Girona (see [9] for more details). Among other sensors, the AUV is endowed with a *Doppler Velocity Log* (DVL) which measures the velocities of the unit with respect to bottom and water, a *Motion Reference Unit* (MRU) that provides absolute attitude data by means of compass and inclinometers, and an MSIS.

The MSIS obtains  $360^\circ$  scans of the environment by rotating a sonar beam through 200 angular steps in about 13.8 seconds. At each angular position, the sensor provides a set of 500 values named *bins*. These values represent a 50 m long echo intensity profile with a resolution of 10 cm. Each of these sets of 500 bins will be referred to as a *beam*. By accumulating this information, an *acoustic image* of the environment can be obtained.

As stated previously, different problems arise when using an MSIS to perform scan-based localization. In order to solve them several processes are necessary. Our proposal is summarized in Figure 1. First, range information is extracted from each MSIS measurement by means of the *beam segmentation*. Also, DVL and MRU readings are fused by means of an *Extended Kalman Filter* (EKF) to obtain *dead reckoning* estimates, as described by [9]. Both the obtained range information and the dead reckoning estimates are stored in two buffers, called *readings history* and *transformations history* respectively. When the MSIS has obtained a  $360^\circ$  view of the environment, the information in these buffers is used by the *scan building* process to compensate the robot motion and build the scan  $S_k$ . Also, the scan builder computes the motion  $x_k$  between the previously gathered

scan and the current one. The scans are stored in the so called *scan history* and the motions are used to augment the SLAM state vector. Afterwards, the new scan  $S_k$  is matched against the scans in the scan history to perform the SLAM state update. This state update exploits the relations between consecutively gathered scans, similarly to the top level in the *Hierarchical SLAM* approach [4]. Finally, the robot pose  $x_R^W$  is computed by the *pose extraction* process.

### A. Beam Segmentation

Our goal is to obtain range scans from the beams as they are provided by the MSIS. Accordingly, the beam segmentation is in charge of computing the distance from the sensor to the largest obstacle in the beam. In some cases, this distance corresponds to the bin with the largest intensity value. However, in some other very frequent situations the distance can not be computed in such way.

To deal with these situations several algorithms have been proposed, tested and evaluated by the authors in [10]. Any of them is able to obtain a much more accurate range scan than a simple maximum intensity selection. However, the details of these algorithms are out of the scope of this paper.

### B. Scan Building

The MSIS data cannot be treated as a synchronous snapshot of the world. Instead, the sonar data is actually acquired whilst the AUV is moving. Thus, the robot motions during the sonar data acquisition have to be taken into account in order to correct the induced distortion. The *scan building* process epitomizes this idea.

The range readings provided by the beam segmentation constitute the range information used to build the scans. Our proposal is to model each measurement in a scan by a normal distribution. In that way, the scans not only hold information about the place where an obstacle has been detected but also about the uncertainty in this detection.

The sonar readings have to be stored in the so called the *readings history*  $RH_t$  so that they can be easily accessed by the scan building process. Similarly, the *transformations history*  $TH_t$  is defined as a history of the most recent  $N$  robot motions.

As the AUV is moving while acquiring the scan, each reading in the  $RH_t$  may have been obtained at a different robot pose. The goal of the scan building process is to represent each reading in one scan with respect to a common coordinate frame. In that sense, each reading in  $RH_t$  can be represented with respect to any coordinate frame referenced in  $TH_t$  while taking into account the robot motion. In this work, the chosen coordinate frame is the central position of the trajectory followed by the robot when collecting the readings involved in the scan, for two main reasons: the similarity to the scans generated by a laser range finder and the reduction of the maximum uncertainty of each reading with respect to the reference frame.

Figure 2-a illustrates the result of the scan builder by the raw range data before and after the scan building. Additionally, 2-b shows the acoustic image corresponding

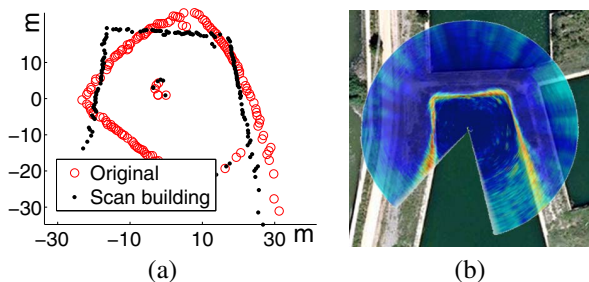


Fig. 2. (a) Range data before and after the scan building process. (b) Acoustic image of one MSIS scan after the scan building process.

to the corrected scan overlaid to a satellite view to show the effects of the correction. More details on how to build the scans, taking into account the robot motion, can be found in [8].

### III. WORLD-CENTRIC TRAJECTORY SLAM

This scan-based approach is based on EKF concepts. The state vector contains the relative positions between consecutively gathered scans.

The robot pose with respect to an earth-fixed coordinate frame could be included in the state vector. However, for the sake of simplicity, a state vector containing only the map is built.

As the map stores relative poses between consecutively obtained scans, the pose of the most recent scan with respect to the robot's starting pose is easily obtained using the  $\oplus$  operator [7]. Additionally, all the information needed to compute the current robot pose with respect to the last scan is available in the transformations history. Using this data the current robot pose with respect to the first robot pose,  $x_R^W$ , can be easily computed by the pose extraction process (see Figure 1).

The measurement update step is performed at the scan level, determining which ones of the stored scans sufficiently overlap with the most recent scan. In order to measure the displacement and rotation between each of the associated scans, a scan matching technique is used. These scan matching estimates constitute the measurements.

The observation function estimates the displacement and rotation from  $S_i$  to  $S_k$  using the state vector. As it explicitly takes into account the whole chain of motions involved in each loop closure, it is possible to correct the whole robot trajectories involved in loops.

By means of the measurements coming from the scan matching, the observation function, as well as the observation matrix, the EKF-SLAM update step can be performed.

However, the effects of the linearizations in the observation model may be problematic especially when closing large loops. In order to alleviate this problem, this proposal uses IEKF [11] instead of EKF. Roughly speaking, the IEKF consists on iterating an EKF and relinearizing the system at each iteration until convergence is achieved. Further details on how to perform this world-centric approach can be found in [8].

The top of figure 3 shows how the map, in the world-centric approach, is built with respect to the world reference

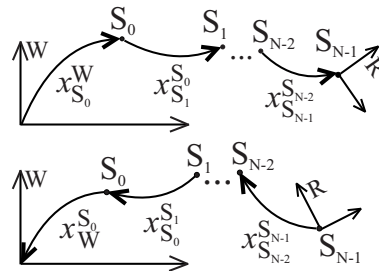


Fig. 3. Relative positions between scans. Top: World-centric. Bottom: Robocentric.

frame. Even though this technique has advantages over the previously existing ones, it is possible to reduce even more the linearization errors and to improve the map consistency, making use of the Robocentric approach, introduced by [7], where the state is represented in a frame relative to the current position of the robot, as it can be seen on the bottom of the figure 3.

### IV. ROBOCENTRIC TRAJECTORY SLAM

The Robocentric Trajectory SLAM is performed at the scan level, and relies on EKF concepts. However, contrarily to the aforementioned world-centric approach [8], the relative positions between consecutively gathered scans are stored in the state vector starting in the current robot pose and ending in a world-fixed coordinate frame, throughout all the gathered scans. Let  $x_k = N(\hat{x}_k, P_k)$  denote the state vector at time step  $k$ :

$$x_k = \begin{bmatrix} x_{S_0}^{S_0} \\ x_{S_1}^{S_0} \\ \vdots \\ x_{S_{k-1}}^{S_{k-2}} \end{bmatrix} \quad (1)$$

where  $x_{S_0}^{S_0}$  denotes the position of the world-fixed coordinate frame  $W$  with respect to firstly gathered scan  $S_0$  and  $x_{S_{i-1}}^{S_{i-1}}$  represents the position of the scan gathered at time step  $i-1$  with respect to the one gathered at time step  $i$ . The items in the state vector constitute the robocentric trajectory. Accordingly, the pose of the world-fixed coordinate frame  $W$  with respect to the robot can be easily computed as  $x_W^{S_k} = x_{S_{k-1}}^{S_{k-1}} \oplus \dots \oplus x_{S_0}^{S_0}$ . Additionally, the robot pose with respect to  $W$  is  $x_W^R = \ominus x_W^{S_k}$ , being  $\oplus$  and  $\ominus$  the compounding and inversion operators [7].

#### A. Prediction

As soon as a new scan  $S_k$  has been gathered, it is stored in the scans history  $SH_k$ . The scans history  $SH_k$  is a buffer containing the range scans gathered up to time step  $k$ . At the same time, the dead reckoning information  $x_{S_k}^{S_{k-1}} = N(\hat{x}_{S_k}^{S_{k-1}}, P_{S_k}^{S_{k-1}})$  is available. The logical step would be to include  $\ominus x_{S_k}^{S_{k-1}}$  as a new feature in the state vector, so that the stored trajectory remains robocentric. However, as dead reckoning (DVL data in our case) is likely to be the less precise component of the system, inverting it at this point would introduce significant linearization error. Our proposal

is, similarly to [2], to delay this inversion until the dead reckoning estimate has been improved by the EKF update step. To this end, the odometric estimate is simply included into the state vector without being inverted. The previously existing items in the state vector remain unaltered, as we assume a static environment:

$$x_k^- = \begin{bmatrix} x_k \\ x_{S_k} \\ x_{S_k-1} \end{bmatrix} \quad (2)$$

### B. Data association

The first step is to determine which ones of the stored scans sufficiently overlap with the most recent scan. Our proposal is to take this decision based on a proximity criteria. Although our implementation uses euclidean distance, other distances could be used.

The displacement and rotation from a scan  $S_i \in SH_k$ , with  $i < k$ , to  $S_k$  can be estimated from the state vector as follows:

$$\delta(i, x_k^-) = \ominus \hat{x}_{S_k}^{S_k-1} \oplus \hat{x}_{S_k-2}^{S_k-1} \oplus \dots \oplus \hat{x}_{S_i}^{S_i+1} \quad (3)$$

Notice that the inversion in this expression is only performed on the mean  $\hat{x}_{S_k}^{S_k-1}$  and, thus, no linearization error appears. The euclidean distance  $d(i, k)$  from the coordinate frame of  $S_i$  to the one of  $S_k$  is the norm of the  $[x, y]$  components of  $\delta(i, x_k^-)$ . The proposal of this paper is, similarly to [12], to select as possible associations those scans in  $SH_k$  that are at an euclidean distance below a certain threshold  $\gamma$ . Let the *associated scans* set  $AS_k$  be defined as the set of possible associations as follows:

$$AS_k = \{i | d(i, k) < \gamma\} \equiv \{a_1, a_2, \dots, a_M\} \quad (4)$$

### C. The measurement model

The proposal of this paper to measure the displacement and rotation between each of the associated scans is the use of scan matching techniques. This paper proposes the use of the *sonar probabilistic Iterative Correspondence* (spIC) because it has shown to be a reliable, stand-alone, scan matching algorithm both using terrestrial ultrasonic range finders [13] and underwater MSIS [14]. Moreover, the spIC has also been successfully applied to underwater SLAM [12]. The explanation of the spIC algorithm is out of the scope of this paper. The reader is directed to the aforementioned studies to have a full description of the algorithm.

The spIC is executed for each  $S_i$  with  $i \in AS_k$  to estimate the displacement and rotation between  $S_i$  and  $S_k$ . The output of the spIC scan matcher constitute the measurements and will be denoted by  $z_k^i$ .

The observation function  $h_k^i$  is in charge of predicting the spIC measurement corresponding to  $S_i$  from the state vector  $x_k^-$ . In other words, the observation function estimates the displacement and rotation from  $S_i$  to  $S_k$  using the state vector. This displacement and rotation has already been computed when selecting associated scans by means of Equation 3. Taking advantage of this makes it possible to spare some CPU time. In other words,  $h_k^i = \delta(i, x_k^-)$ .

As this observation function explicitly takes into account the whole chain of motions involved in each loop closure, the proposed approach is able to correct the whole robot trajectory involved in loops.

The observation matrix  $H_k^i$ , which is defined as the Jacobian matrix of  $h_k^i$ , is the following:

$$H_k^i = \left. \frac{\partial h_k^i}{\partial x_k^-} \right|_{\hat{x}_k^-} = \left[ \frac{\partial h_k^i}{\partial x_W^{S_0}} \dots \frac{\partial h_k^i}{\partial x_{S_{i-1}}^{S_i}} \dots \frac{\partial h_k^i}{\partial x_{S_k}^{S_k-1}} \right] \Bigg|_{\hat{x}_k^-} \quad (5)$$

It is easy to see that only the terms depending on the state vector components  $x_{S_{i-1}}^{S_i}$  to  $x_{S_k-2}^{S_k-1}$  and  $x_{S_k}^{S_k-1}$  are non-zero. The non-zero term that depends on  $x_{S_k}^{S_k-1}$  is:

$$\begin{aligned} \left. \frac{\partial h_k^i}{\partial x_{S_k}^{S_k-1}} \right|_{\hat{x}_k^-} &= \left. \frac{\partial h_k^i}{\partial \ominus x_{S_k}^{S_k-1}} \right|_{\hat{x}_k^-} \cdot \left. \frac{\partial \ominus x_{S_k}^{S_k-1}}{\partial x_{S_k}^{S_k-1}} \right|_{\hat{x}_k^-} \\ &= J_{1\oplus} \{ \ominus x_{S_k}^{S_k-1}, x_{S_k}^{S_k-1} \oplus h_k^i \} \cdot J_{\ominus} \{ x_{S_k}^{S_k-1} \} \end{aligned} \quad (6)$$

where  $J_{1\oplus}$  is the first Jacobian matrix of the compounding operator and  $J_{\ominus}$  is the Jacobian matrix of the inversion, as described in [7]. The remaining non-zero terms of  $H_k^i$  are the following:

$$\begin{aligned} \left. \frac{\partial h_k^i}{\partial x_{S_j}^{S_j+1}} \right|_{\hat{x}_k^-} &= \left. \frac{\partial h_k^i}{\partial g_{j,i}} \right|_{\hat{x}_k^-} \cdot \left. \frac{\partial g_{j,i}}{\partial x_{S_j}^{S_j+1}} \right|_{\hat{x}_k^-} \\ &= J_{1\oplus} \{ g_{j,i}, \ominus g_{j,i} \oplus h_k^i \} \cdot J_{2\oplus} \{ g_{j,i} \ominus x_{S_j}^{S_j+1}, x_{S_j}^{S_j+1} \} \end{aligned} \quad (7)$$

where  $i \leq j \leq k-2$  and  $g_{j,i}$ , which is defined just to ease notation, is  $g_{j,i} = x_{S_k}^{S_k-1} \oplus x_{S_k-2}^{S_k-1} \oplus \dots \oplus x_{S_j}^{S_j+1}$ .  $J_{2\oplus}$  is the second Jacobian matrix of the compounding operator, also described in [7].

At this point, the measurements  $z_k^i$  coming from the scan matching and the observation function  $h_k^i$ , as well as the observation matrix  $H_k^i$  are available for all  $i \in AS_k$ . The measurement vector  $z_k$ , the observation function  $h_k$  and the observation matrix  $H_k$ , which are used by in the EKF update, can be constructed as follows:

$$z_k = \begin{bmatrix} z_k^{a_1} \\ \vdots \\ z_k^{a_M} \end{bmatrix} \quad h_k = \begin{bmatrix} h_k^{a_1} \\ \vdots \\ h_k^{a_M} \end{bmatrix} \quad H_k = \begin{bmatrix} H_k^{a_1} \\ \vdots \\ H_k^{a_M} \end{bmatrix} \quad (8)$$

where  $a_1, a_2, \dots, a_M$  denote the items in  $AS_k$  (see Equation 4).

### D. Update

By means of  $z_k$ ,  $h_k$  and  $H_k$  the EKF-SLAM update step can be performed. However, the effects of the linearizations in the observation model may be problematic especially when closing large loops. In order to alleviate this problem, our proposal is not to use an EKF but an IEKF [11]. Roughly speaking, the IEKF consists on iterating an EKF and relinearizing the system at each iteration until convergence is achieved.

At iteration  $j$ , the mean and the associated covariance matrix obtained from IEKF are:

$$P_k^j = P_k^- - P_k^- H_{k,j}^T (H_{k,j} P_k^- H_{k,j}^T + P_{spIC,k})^{-1} \cdot H_{k,j} P_k^- \quad (9)$$

$$\hat{x}_k^{j+1} = \hat{x}_k^j + P_k^j H_{k,j}^T P_{spIC,k}^{-1} (z_k - h_k) - P_k^j (P_k^-)^{-1} (\hat{x}_k^j - \hat{x}_k^-) \quad (10)$$

where  $H_{k,j}$  denotes the observation matrix  $H_k$  evaluated at  $\hat{x}_k^j$  (i.e. each  $H_k^i$  in Equation 5 is evaluated at the value of the state vector in the previous IEKF iteration). The term  $P_{spIC,k}$  is a block diagonal matrix containing the scan matching covariances corresponding to the items in  $z_k$ . When the IEKF achieves convergence, the state vector in the last iteration constitutes the updated state  $x_k^+$ .

It is important to emphasize that this step only updates the items in the state vector involved in the detected loops. Thus, the matrix  $H$  in Equation 8 could be reduced by removing all the zero valued columns on the left side of the matrix and then updating only the part of the state vector involved in all the detected loops. Moreover, the presented update step makes it possible to store different loops when they are detected and close them later simultaneously, not necessarily at each SLAM step [4]. Thanks to this, the loop closure can be delayed if the computational resources are not available at a certain time step. Also, the overall computational cost is reduced because, prior to the loop closing, the newly gathered scans are independent and those parts of the covariance matrix related to the new scans are block diagonal.

### E. Inversion

The dead reckoning estimate which was included in the state vector during the prediction step has now been improved thanks to the IEKF update. Thus, now it should be inverted so that the state vector remains robocentric. The resulting state vector is:

$$x_{k+1} = \begin{bmatrix} x_W^{S_0} \\ \vdots \\ x_{S_{k-1}}^{S_{k-1}} \\ \ominus x_{S_k}^{S_{k-1}} \end{bmatrix} \quad (11)$$

The obtention of the mean  $\hat{x}_{k+1}$  of the state vector is straightforward. In order to obtain the covariance  $P_{k+1}$ , the following Jacobian matrix has to be computed:

$$\left. \frac{\partial x_{k+1}}{\partial x_k^+} \right|_{\hat{x}_k^+} = \left[ \begin{array}{cccc} \frac{\partial x_W^{S_0}}{\partial x_W^{S_0}} & \frac{\partial x_W^{S_0}}{\partial x_{S_0}^{S_1}} & \cdots & \frac{\partial x_W^{S_0}}{\partial x_{S_k}^{S_{k-1}}} \\ \vdots & \vdots & \ddots & \vdots \\ \frac{\partial \ominus x_{S_k}^{S_{k-1}}}{\partial x_W^{S_0}} & \frac{\partial \ominus x_{S_k}^{S_{k-1}}}{\partial x_{S_0}^{S_1}} & \cdots & \frac{\partial \ominus x_{S_k}^{S_{k-1}}}{\partial x_{S_k}^{S_{k-1}}} \end{array} \right] \Bigg|_{\hat{x}_k^+} \quad (12)$$

It is easy to see that this matrix actually is:

$$J \equiv \left. \frac{\partial x_{k+1}}{\partial x_k^+} \right|_{\hat{x}_k^+} = \begin{bmatrix} I_{3k \times 3k} & 0_{3k \times 3} \\ 0_{3 \times 3k} & J_{\ominus \{ \hat{x}_{S_k}^{S_{k-1}} \}} \end{bmatrix} \quad (13)$$

Using this matrix, the state covariance can be updated as  $P_{k+1} = J \cdot P_k \cdot J^T$ .

## V. EXPERIMENTAL RESULTS

The experimental data used to validate our underwater SLAM approach was obtained by [9] in an abandoned marina situated near St. Pere Pescador in the Costa Brava (Spain). A satellite view of this environment is available in [15]. The Ictineu AUV was teleoperated along a 600m trajectory at an average speed of 0.2m/s. The trajectory includes a small loop as well as a 200m long straight path. The gathered data included measurements from the DVL, the MRU and the MSIS. Additionally, a buoy with a GPS was attached to the robot in order to obtain the ground truth.

Figure 4-a shows the trajectories provided by dead reckoning (DVL+MRU) and the GPS. Also, the sonar readings are plotted according to the dead reckoning trajectory for visual inspection. The problems of dead reckoning can be appreciated. For example, the entrance to the canal is misaligned (i.e. the loop is not closed) due to the drift error.

In order to show the advantages of the Robocentric Trajectory approach, the World-centric Trajectory [8] approach has also been implemented. In the world-centric approach, the relative motions between consecutively gathered scans are stored starting in the first robot pose and ending in the current one throughout all the poses where the scans have been gathered. Because the world-centric approach stores local robot motions, similarly to the proposal in this paper, it also introduces significantly less linearization errors than the standard EKF approach, where absolute landmark positions are used.

The results provided by the World-centric Trajectory SLAM are shown in Figure 4-b together with the ground truth provided by the GPS. It can be observed how this approach provides a trajectory very similar to the ground truth, especially before entering the canal where some loop closures have been performed. However, after more than 200 meters without revisiting known areas, the pose error surpasses the 6m. The ellipses shown in Figure 4-b correspond to the  $2\sigma$  bounds for some scans positions with respect to the first robot pose after the whole World-centric Trajectory SLAM process. It can be observed that the  $2\sigma$  bounds are smaller on the left side of the image where different loop closures are performed.

The results corresponding to the Robocentric Trajectory SLAM discussed in this paper are shown in Figure 4-c. Similarly to the aforementioned approach, the process clearly provides results very close to the ground truth. However, the results in the canal, when no loops can be closed, are significantly better in this case.

The main differences between both approaches arise when no loop closures are available. This can be clearly appreciated in Figure 4-d, where the evolution of the pose error with

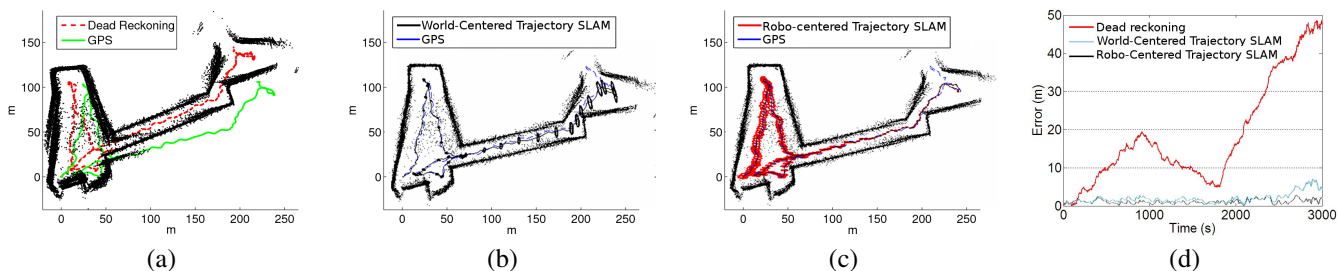


Fig. 4. (a) Trajectories according to dead reckoning and GPS. Sonar readings positioned according to dead reckoning. (b) Trajectories according to World-centric Trajectory SLAM and GPS. Sonar readings positioned according to SLAM. (c) Trajectories according to Robocentric Trajectory SLAM and GPS. Sonar readings positioned according to SLAM. (d) The dead reckoning and SLAM errors.

	Loop	No loop	Global
Robocentric	0.99m	1.51m	1.15m
World-centric	1.49m	3.3m	2.05m

TABLE I  
MEAN ERRORS FOR WORLD-CENTRIC AND ROBOCENTRIC  
TRAJECTORIES

time is shown. The pose error is defined here as the distance between a pose estimation and the corresponding ground truth. It can be observed that the main differences between World-centric Trajectory and Robocentric Trajectory, as well as dead reckoning, appear, approximately, from the 1800 seconds onwards.

Table I emphasizes these differences by showing the mean errors in the loops area and in the canal area, as well as the global mean error. The robocentric trajectory approach mainly reduces the linearization errors when matching scans that have been gathered close in time. As this is the most common situation when no loops appear, that is why the main differences appear in the canal area.

## VI. CONCLUSIONS

This paper proposes a novel approach to perform underwater SLAM using a MSIS. The presented approach starts by processing the underwater sonar data so that range information is extracted from the acoustic profiles. Also, the range data is grouped in scans while taking into account that the robot moves during the sonar data gathering. Afterwards, the scans are stored and the relative robot motions between consecutively gathered scans are included in the state vector. Thus, SLAM is performed using the whole sequence of robot motions where scans have been gathered. Moreover, this sequence is stored starting in the current robot pose, so that EKF linearization errors can be reduced, similarly to the robocentric SLAM approach.

Different experiments have been performed, comparing the robocentric trajectory approach with a world-centric trajectory method. Results have shown the accuracy of the method, providing a mean pose error of 1.15m after a 600m underwater mission.

## VII. ACKNOWLEDGMENTS

The authors are grateful to the members of the Underwater Robotics Lab, in Universitat de Girona, for the data sets and the useful advice.

## REFERENCES

- [1] H. Durrant-Whyte and T. Bailey, "Simultaneous localization and mapping (SLAM): part I," *IEEE Robotics and Automation Magazine*, vol. 13, no. 2, pp. 99–110, June 2006.
- [2] J. Castellanos, J. Neira, and J. Tardós, "Limits to the consistency of EKF-based SLAM," in *Proceedings of the 5th IFAC/EURON Symposium on Intelligent Autonomous Vehicles*, July 2004.
- [3] S. Thrun, W. Burgard, and D. Fox, *Probabilistic Robotics*. The MIT Press, 2005.
- [4] C. Estrada, J. Neira, and J. D. Tardós, "Hierarchical SLAM: real-time accurate mapping of large environments," *IEEE Transactions on Robotics*, vol. 21, no. 4, pp. 588–596, August 2005.
- [5] S. Williams, G. Dissanayake, and H. Durrant-Whyte, "An efficient approach to the simultaneous localisation and mapping problem," in *Proceedings of the IEEE International Conference on Robotics and Automation (ICRA)*, vol. 1, February 2002, pp. 406–411.
- [6] R. Martinez-Cantin and J. Castellanos, "Bounding uncertainty in ekf-slam: the robocentric local approach," in *Robotics and Automation, 2006. ICRA 2006. Proceedings 2006 IEEE International Conference on*, May 2006, pp. 430–435.
- [7] J. Castellanos, R. Martinez-Cantin, J. Tardós, and J. Neira, "Robocentric map joining: Improving the consistency of ekf-slam," *Robotics and Autonomous Systems*, vol. 55, pp. 21–29, 2007.
- [8] A. Burguera, G. Oliver, and Y. González, "Scan-based slam with trajectory correction in underwater environment," in *Proceedings of the IEEE/RSJ International Conference on Intelligent Robots and Systems (IROS'10)*, Taipei (Taiwan), 2010.
- [9] D. Ribas, P. Ridao, J. Tardós, and J. Neira, "Underwater SLAM in man made structured environments," *Journal of Field Robotics*, vol. 11-12, no. 25, pp. 898–921, 2008.
- [10] A. Burguera, G. Oliver, and Y. González, "Range extraction from underwater imaging sonar data," in *Proceedings of the IEEE International Conference on Emerging Technologies and Factory Automation (ETFA'10)*, Bilbao (Spain), 2010.
- [11] Y. Bar-Shalom, X. Rong Li, and T. Kirubarajan, *Estimation with applications to tracking and navigation: theory algorithms and software*. John Wiley and Sons, Inc., 2001.
- [12] A. Mallios, P. Ridao, E. Hernandez, D. Ribas, F. Maurelli, and Y. Petillot, "Pose-based slam with probabilistic scan matching algorithm using a mechanical scanned imaging sonar," in *Proceedings of Oceans 2009-Europe*, May 2009, pp. 1–6.
- [13] A. Burguera, Y. González, and G. Oliver, "A probabilistic framework for sonar scan matching localization," *Advanced Robotics*, vol. 22, no. 11, pp. 1223–1241, 2008.
- [14] A. Burguera, Y. González, and G. Oliver, "Underwater scan matching using a mechanical scanned imaging sonar," in *Submitted to Proceedings of Intelligent Autonomous Vehicles*, 2010.
- [15] Google Maps, "St. Pere Pescador, Abandoned Marina. <http://maps.google.es/maps?hl=es&ie=UTF8&ll=42.202645,3.10662&spn=0.005182,0.008862&t=h&z=17>," Accessed 12-March-2011.